
Vibrational spectroscopic study of tetracalcium phosphate in pure polycrystalline form and as a constituent of a self-setting bone cement

U. Posset,¹ E. Löcklin,¹ R. Thull,¹ W. Kiefer²

¹Lehrstuhl und Abteilung für Experimentelle Zahnmedizin, Klinik und Poliklinik für Zahn-, Mund- und Kieferkrankheiten, Universität Würzburg, Pleicherwall 2, D-97070 Würzburg, Germany

²Institut für Physikalische Chemie, Universität Würzburg, Am Hubland, D-97074 Würzburg, Germany

Received 28 May 1997; accepted 11 September 1997

Abstract: Polycrystalline tetracalcium phosphate (TTCP), a material of considerable interest for human implantation due to its similarity to hydroxyapatite, was studied by means of Raman and FT-IR spectroscopy. The spectra were interpreted on the basis of group theoretical considerations. In addition, the setting reaction of a calcium phosphate cement (CPC) consisting of an equimolar mixture of TTCP and dicalcium phosphate (DCPA) was investigated by Raman spectroscopy. The band of the totally symmetric phosphate mode ν_1 of TTCP showed marked factor group splittings. The splitting components arose at coincident wave numbers in the IR and Raman spectra. This observation was in accor-

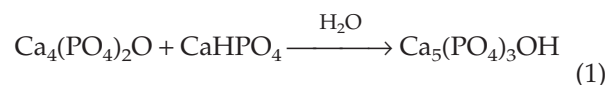
dance with space group $P2_1$ (factor group C_2^2 , $Z = 4$). The characteristic splitting of ν_1 allowed the setting reaction of CPC to hydroxyapatite to be followed. According to the Raman spectroscopic results, considerable amounts of TTCP must be present at the sample surface after 24 h of setting in an aqueous environment. © 1998 John Wiley & Sons, Inc. *J Biomed Mater Res*, **40**, 640–645, 1998.

Key words: tetracalcium phosphate; calcium phosphate cement; Raman spectroscopy; FT-IR spectroscopy; setting reaction

INTRODUCTION

Tetracalcium phosphate (TTCP), $\text{Ca}_4(\text{PO}_4)_2\text{O}$, is the calcium phosphate with the highest Ca/P ratio and hence the highest basicity. Due to its structural and chemical similarity to hydroxyapatite (HA), the main component of human and animal hard tissue, interest in the material as an implantable biomaterial has been growing. TTCP shows only low *in vivo* resorption rates, and its adhesion to bone tissue is comparable to hydroxyapatite. It is supposed that TTCP plays an important role in biological calcification processes, its biocompatibility being comparable to that of HA.¹ Nevertheless, owing to its nontrivial synthesis via a high-temperature solid-state reaction, tetracalcium phosphate has been physically and physico-chemically characterized only to a minor extent. A systematic investigation and interpretation of its vibrational spectra are still missing.

The discovery that the basic TTCP reacts with acid dicalcium phosphate anhydrous CaHPO_4 (DCPA) to form pure hydroxyapatite, according to Equation (1), led to the development of a novel self-setting calcium phosphate cement (CPC) by Brown and Chow in 1985.²



The combination of self-setting, molding, biocompatibility, and the lack of any by-products makes CPC a promising material for dental and orthopedic applications.³ Calcium phosphate cement is indicated mainly in cases of cranial defects and orbital and frontofacial reconstructions.^{4–7}

The intention of this study was by means of Raman and FT-IR spectroscopy to characterize tetracalcium phosphate both in pure polycrystalline form and as a constituent of calcium phosphate cement. Solid-state splittings were interpreted on the basis of group theoretical considerations and were utilized to follow the cement setting reaction kinetics.

Correspondence to: Dr. U. Posset
Contract grant sponsor: Fonds der Chemischen Industrie

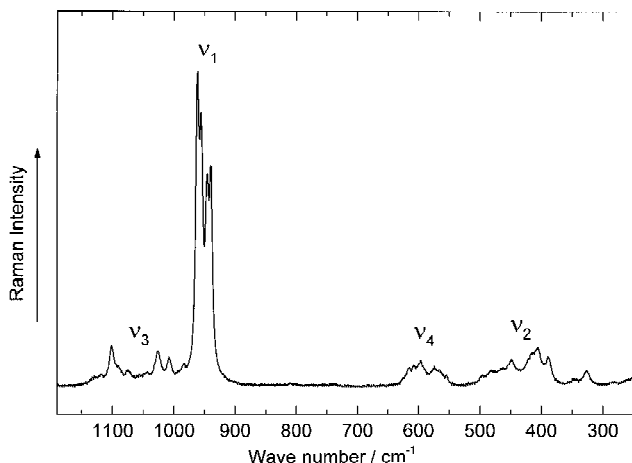


Figure 1. Raman spectrum of polycrystalline tetracalcium phosphate. Excitation wave length $\lambda_0 = 514.5$ nm, power at sample $P = 25$ mW, OMA detection.

MATERIALS AND METHODS

Synthesis of tetracalcium phosphate

Equimolar amounts of calcium carbonate (CC) flux grade (J. T. Baker) and previously dried dicalcium phosphate anhydrous (DCPA, J. T. Baker) were ground by mortar and pestle and stirred in doubly distilled water for 20 h in order to obtain a homogeneous mixture. An alumina crucible was filled with the dried mixture, annealed to 1500°C with a rate of 10°C/min, and held at this temperature for 6 h. The product rapidly was cooled to room temperature by means of a lifting device. Rapid cooling was essential in order to prevent formation of HA and calcium oxide, a side reaction taking place between 800° and 1250°C in moist atmospheres.⁸ The product was characterized by EDX analysis and powder X-ray diffraction to confirm phase purity. It was maintained in anhydrous atmosphere.

Synthesis of calcium phosphate cement (CPC)

The solid phase of calcium phosphate cement was prepared according to the procedure given by Fukase et al.⁹ As liquid phase *aqua injectabilia* was used. In order to obtain a kneadable consistency, a powder-to-solid ratio of 3.3/1 was chosen. After an initial mixing time of 30 s, the paste was pressed into a sample holder with a circular nut according to reference.¹⁰ The sample then was maintained at 37°C and 100% humidity.

Spectroscopic measurements

For excitation of Raman spectra the 514.5 nm line (50 mW) of an Ar⁺-ion laser (Spectra Physics 2016) and the 647.1 nm line (200 mW) of a Kr⁺-ion laser (Spectra Physics 2020) were

used. In the case of 514.5 nm excitation, a triple monochromator (Dilor X-Y) equipped with an optical multichannel analyzer (OMA) was applied. Laser and Raman scattering were focused by means of a micro-Raman setup described by Lankers et al.¹¹ A double monochromator SPEX model 1404 and a CCD (charge coupled device) system Photometrics model CCD 9000, were used for dispersion and detection of spectra obtained by means of the 647.1 nm line. The rotating-surface-scanning technique reported by Zimmerer and Kiefer was applied in this case.¹⁰ Raman spectra of the setting cement were measured *in situ*, in the sample holder mentioned above. Spectral resolution was 2 cm⁻¹ if not otherwise stated. FT-IR spectra were recorded from KBr pellets by means of a Nicolet 320 FT-IR spectrometer with a spectral resolution of 2 cm⁻¹.

RESULTS AND DISCUSSION

Vibrational spectrum of polycrystalline TTCP

In 1983 Bertoluzza et al. published some vibrational data on TTCP for comparison purposes. However, they did not make any assignments or discuss the solid-state effects obviously present.¹² Figures 1 and 2 show the Raman and FT-IR spectra of pure polycrystalline TTCP in survey. The corresponding wave numbers are compiled in Table I. In general, the spectra consisted of bands due to lattice vibrations of Ca²⁺ and O²⁻-ions (below 350 cm⁻¹) and those originating from the vibrational modes of the phosphate ions, ν_1 - ν_4 (see Table II).¹³

The Raman spectrum of TTCP was dominated by the band of the totally symmetric stretching vibration ν_1 (A_1) in the range between 961 and 940 cm⁻¹. The threefold degenerate stretching mode ν_3 (T_2) gave rise to

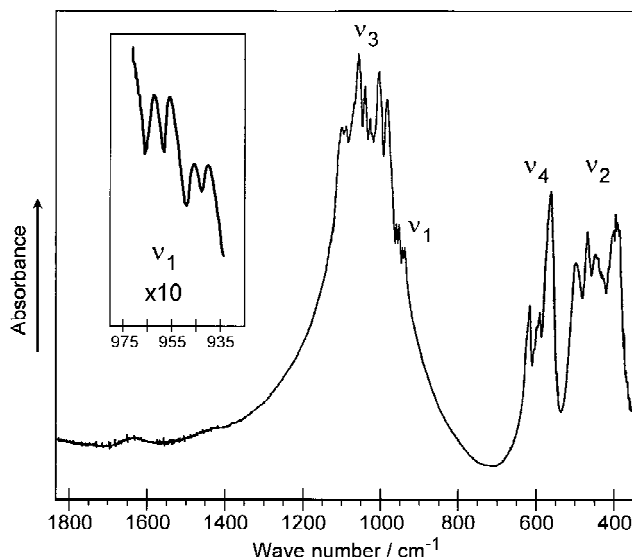


Figure 2. FT-IR spectrum of polycrystalline tetracalcium phosphate in KBr.

TABLE I
Vibrational Wave Numbers [cm^{-1}] of Polycrystalline
Tetracalcium Phosphate

Raman $\lambda_0 = 514.5 \text{ nm}$	FT-IR KBr	Assignment
1119 vw		
1101 w	1105 w	
1091 sh	1093 w	
1076 vw	1073 w	
	1062 s	ν_3 , threefold degenerate
1045 vw	1046 s	stretching mode
1026 w	1033 m	
1008 w	1010 s	
983 vw	989 s	
961 vs	962 w	
956 vs	956 w	
946 s	946 w	ν_1 , symmetric stretching mode
940 s	941 w	
615 vw	620 w	
608 vw		
597 w	594 w	
576 vw	571 s	ν_4 , threefold degenerate
566 sh		deformational mode
556 vw		
495 sh	501 w	
481 sh	471 m	
463 sh		
449 w	450 w	ν_2 , twofold degenerate
414 sh	429 w	deformational mode
407 w		
389 w	399 m	
346 vw		
324 w		
249 vw?		lattice modes
218 vw?		
208 vw?		

a crowd of weak bands between 983 and 1119 cm^{-1} , located on the high wave number side of the ν_1 pattern. In the IR spectrum the situation was complementary. An intense broad band around 1010 cm^{-1} , showing many shoulders, due to ν_3 , and only weak IR absorptions arising from ν_1 between 962 and 941 cm^{-1} , located at the low wave number end of the ν_3 absorption, was observed. The degenerate deformational modes ν_2 (E) and ν_4 (T_2) gave rise to two isolated band patterns between 556 and 620 cm^{-1} and between 389 and 501 cm^{-1} , respectively, with medium intensity, both in the infrared and the Raman spectra. Essentially, all phosphate vibrational bands were observed

TABLE II
Vibrational Wave Numbers of the PO_4^{3-} -ion in Aqueous
solution

T_d	Wave number [cm^{-1}]			
	ν_1 (A_1)	ν_2 (E)	ν_3 (T_2)	ν_4 (T_2)
PO_4^{3-}	938	420	1017	567

TABLE III
Correlation Table for a Phosphate Ion Under Space
Group $P2_1$

	Free Ion T_d	Site Group C_1	Factor Group C_2^2
ν_1	A_1 [Ra]	A [IR, Ra]	2A [IR, Ra] + 2B [IR, Ra]
ν_2	E [Ra]	2A [IR, Ra]	2 (2A [IR, Ra] + 2B [IR, Ra])
ν_3, ν_4	T_2 [IR]	3A [IR, Ra]	3 (2A [IR, Ra] + 2B [IR, Ra])

Spectral activity in brackets.

in both the Raman and IR spectra. All band positions were found to be coincident. This should be stated especially for the ν_1 stretching mode, the four components of which were recognized to be present at identical wave numbers in the Raman and the IR spectra for the first time (see detail in Fig. 2).

Structure and factor group analysis of TTCP

Although the band patterns of TTCP can be correlated to the normal modes of the phosphate ion of symmetry T_d , for successful interpretation of band numbers and spectral activities, spectra must be analyzed in terms of factor group symmetry.¹⁴ The factor group splittings of TTCP provided structural information due to their close relation to crystal or unit cell symmetries. Determination of the TTCP space group was not straightforward. Single crystal X-ray diffraction measurements revealed space group $P2_1$ (factor group C_2^2 , formula units per unit cell $Z = 4$) to be present although other space groups were discussed, among which only $P2_1/m$ (C_{2h}^2 , $Z = 4$) should be mentioned here.^{15,16} $P2_1$ and $P2_1/m$ are different only in a mirror plane. In Tables III and IV, according to the two corresponding factor group symmetries C_2^2 and C_{2h}^2 , vibrational species of free tetrahedral phosphate ions correlate with those of vibrationally coupled phosphate ions in TTCP. The most apparent splitting was shown by the ν_1 phosphate band, which consisted of a characteristic pattern of four bands of similar intensity (Fig. 3, Table V). The pattern was unchanged even at a sample temperature of 18 K; no more than four components could be resolved. The corresponding IR absorption profile of ν_1 was observed at coincident wave

TABLE IV
Correlation Table for a Phosphate Ion Under Space
Group $P2_1/m$

	Free Ion T_d	Site Group C_1	Factor Group C_{2h}^2
ν_1	A_1 [Ra]	A [IR, Ra]	$A_{g'} B_g$ [Ra] + $A_{u'} B_u$ [IR]
ν_2	E [Ra]	2A [IR, Ra]	2 ($A_{g'} B_g$ [Ra] + $A_{u'} B_u$ [IR])
ν_3, ν_4	T_2 [IR]	3A [IR, Ra]	3 ($A_{g'} B_g$ [Ra] + $A_{u'} B_u$ [IR])

Spectral activity in brackets.

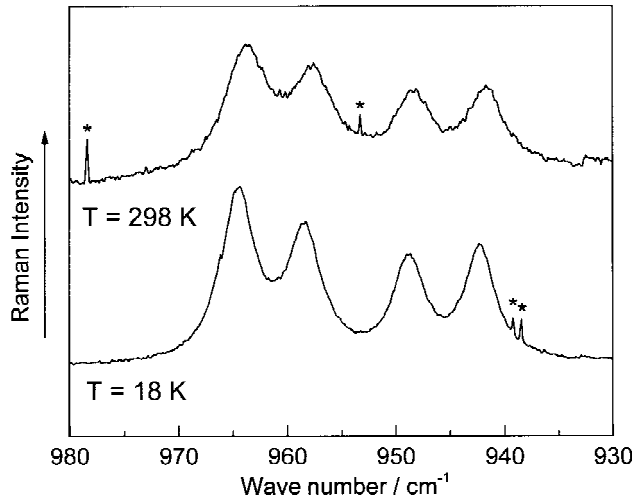


Figure 3. The ν_1 band of polycrystalline tetracalcium phosphate at ambient and low sample temperature. $\lambda_0 = 647.1$ nm, $P = 200$ mW, CCD detection, spectral resolution $s = 0.15$ cm^{-1} . Asterisks indicate artefacts.

numbers. These observations were in agreement with the predictions made for space group $P2_1$ (factor group C_2^2), that is, splitting into four components $2A + 2B$, all Raman and IR active (Table III). The rule of mutual exclusion, that is, exclusive spectral activity of gerade and ungerade modes in the Raman or IR spectra, respectively, did not apply (Table IV). Therefore, the centrosymmetric space group $P2_1/m$ could be excluded by theory. The degenerate stretching mode ν_1 and deformational modes ν_2 and ν_4 also showed, beneath the site symmetry related removal of degenerations, marked factor group splittings, which gave rise to extensive band structures of about 50 (ν_4 : 620 to 556 cm^{-1}) to over 100 wave numbers (ν_2 : 501 to 389 cm^{-1} , ν_3 : 1119 to 983 cm^{-1}) broad. The extremely strong ν_3 absorption clearly dominated the IR spectrum of TTCP. According to the correlation for $P2_1$ in Table III, ν_2 - ν_4 were expected to consist of eight (ν_2) or twelve (ν_3 , ν_4) components. Predicted and observed numbers of bands did not agree, except for ν_1 . This may have been due to superimposed or hidden bands, or bands of very low intensity. However, the maximum number of components permissible by symmetry restrictions was not exceeded in any case. For more detailed analysis, single crystal measurements become inevitable.

TABLE V
Components of the ν_1 Mode of TTCP Recorded at Ambient and Low Temperature With Enhanced Spectral Resolution

Temperature [K]	Peak 1	Peak 2	Peak 3	Peak 4
18	942.2	948.7	958.5	964.5
298	942.0	948.7	958.0	963.9

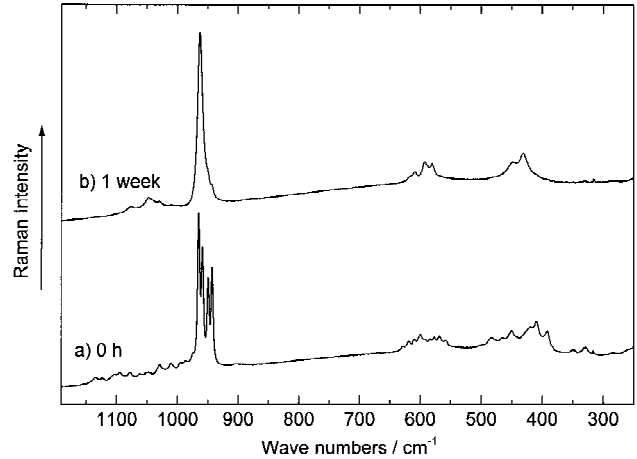


Figure 4. Raman spectra of calcium phosphate cement (CPC). Spectrum a: unset cement; spectrum b: set cement after 1 week immersion time. $\lambda_0 = 647.1$ nm, $P = 200$ mW, CCD detection.

Raman spectrum of calcium phosphate cement

Fukase et al. studied the cement reaction of CPC [Eq. (1)] by means of quantitative X-ray diffractometry. Their results showed that HA of low crystallinity was the only reaction product and that about 90% of

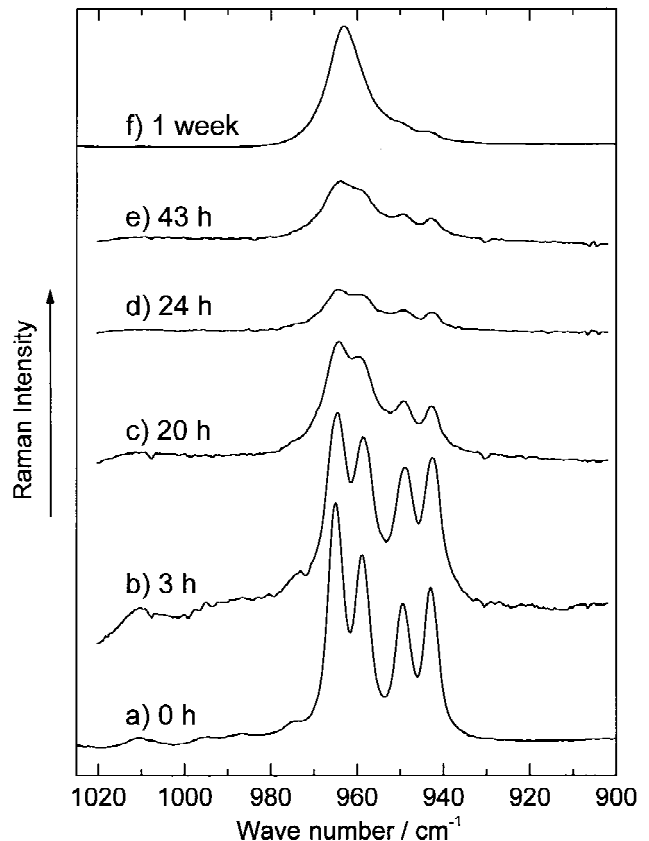


Figure 5. The $\nu_1(\text{PO}_4)$ band of CPC during the setting reaction. Immersion times indicated. $\lambda_0 = 647.1$ nm, $P = 200$ mW, CCD detection.

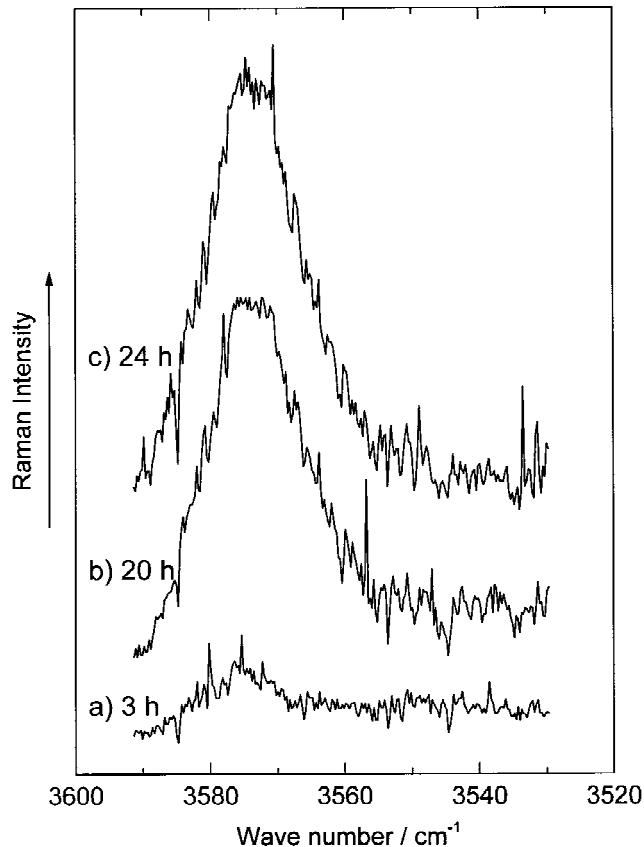


Figure 6. The $\nu(\text{OH})$ band of CPC during the setting reaction. Immersion times indicated. $\lambda_0 = 647.1 \text{ nm}$, $P = 200 \text{ mW}$, CCD detection.

the cement was converted to HA after 4 h.⁹ In the present study, the reaction of CPC to HA was followed by means of Raman spectroscopy in order to obtain further information about the setting kinetics. In Figure 4, the Raman spectra of unset CPC-Paste (spectrum a) and the set material (spectrum b) are displayed. Obviously, spectrum a is identical to that of TTCP. It is supposed that the intensities of PO_4^{3-} Raman bands in TTCP are superior to those of the less symmetric HPO_4^{2-} ion in DCPA. As a consequence, the DCPA lines simply would be superimposed. The spectrum of CPC was suitable for studying conversion of TTCP by means of ν_1 . Spectrum b was observed after setting in 100% humidity at 37°C for one week, after which time only HA bands could be found.¹⁷ The relatively high band widths in spectrum b resulted from the low crystallinity of the set cement. Raman spectra of the sample obtained in the ν_1 domain at various time intervals are shown in Figure 5. After 3 h of setting, no change was observed (spectrum b). After 20 h the band shape significantly changed, but the four-band pattern of TTCP still was present (spectrum c). According to spectrum e, the cement even contained a considerable amount of TTCP after 43 h. Total conversion of CPC to HA was seen after several days.

If HA formed, a hydroxyl vibrational band was expected to arise. In Figure 6, the Raman spectra in the $\nu(\text{OH})$ region are given at various time intervals. The $\nu(\text{OH})$ band of set CPC was observed at 3573 cm^{-1} . This value was identical to that reported for polycrystalline, stoichiometric hydroxyapatite prepared by a high-temperature procedure.¹⁷

In contrast to the results obtained by Fukase et al., significant conversion could not be deduced from the present Raman spectroscopic results until about 20 h. This temporal discrepancy might be explained by the different analytical techniques used. In order to obtain powder diffractograms, samples had to be ground. Consequently, the information obtained from X-ray powder diffractometry was averaged over the sample volume. In this study the setting sample was left intact and placed inside the sample holder. Considering that Raman spectra provided information only from the focal region, and the laser was focused onto the sample surface, the information obtained must have originated from a superficial layer several hundred micrometers thick. Probably, the acidic, more soluble component of DCPA was leached out to some extent so that conversion of CPC was slowed, especially at the surface. Later on, hydration of the superficially remaining TTCP to HA occurred.¹⁸ This hypothesis was confirmed recently by SEM observations of TTCP domains remaining on the surfaces of CPC samples after 24 h of setting (U. Posset and R. Thull, unpublished results).

We thank Mrs. C. Fickert and Dr. J. Popp for technical assistance, and helpful suggestions by Mr. J. Probst are gratefully acknowledged.

References

1. C. P. A. T. Klein, P. Patka, J. G. C. Wolke, J. M. A. de Blicke-Hogervorst, and K. de Groot, "Long-term *in vivo* study of plasma-sprayed coatings on titanium alloys of tetracalcium phosphate, hydroxyapatite, and α -tricalcium phosphate," *Biomaterials*, **5**, 146–150 (1994).
2. W. E. Brown and L. C. Chow, "A new calcium phosphate, water-setting cement," in *Cement Research Progress*, P. W. Brown (ed.), American Ceramic Society, Westerville, Ohio, 1986, pp. 351–379.
3. S. E. Gruninger, C. Siew, L. C. Chow, and A. O'Young, "Evaluation of the biocompatibility of a new calcium phosphate setting cement," *J. Dent. Res.*, **63**, 200 [Abstract No. 270], (1984).
4. A. Sugawara, L. C. Chow, L. C. Takagi, and H. Chohayeb, "In vitro evaluation of the sealing ability of a calcium phosphate cement as a root canal sealer-filler," *J. Endodont.*, **16**, 162–165 (1990).
5. J. H. Lu, C. Siew, and P. J. Robinson, "New attachment following the use of a novel calcium phosphate system," *J. Dent. Res.*, **67**, 352 [Abstr. No. 1913] (1990).
6. C. D. Friedman, P. D. Constantino, K. Jones, L. C. Chow, H. J. Pelzer, and G. A. Sisson, Sr., "Hydroxyapatite cement. II. Oblit-

- eration and reconstruction of the cat frontal sinus," *Arch. Otolaryngol. Head Neck Surg.*, **117**, 385–389 (1991).
7. P. D. Constantino, C. D. Friedman, K. Jones, L. C. Chow, H. J. Pelzer, and G. A. Sisson, Sr., "Experimental hydroxyapatite cement cranioplasty," *Plast. Reconstr. Surg.*, **90**, 174–185 (1992).
 8. H. Monma, M. Goto, H. Nakajima, and H. Hashimoto, "Preparation of tetracalcium phosphate," *Gypsum Lime*, **202**, 151–155 (1986).
 9. Y. Fukase, E. D. Eanes, S. Takagi, L. C. Chow, and W. E. Brown, "Setting reactions and compressive strengths of calcium phosphate cements," *J. Dent. Res.*, **69**, 1852–1856 (1990).
 10. N. Zimmerer and W. Kiefer, "Rotating surface scanning technique for Raman spectroscopy," *Appl. Spectrosc.*, **28**, 279–281 (1974).
 11. M. Lankers, D. Göttges, A. Materny, K. Schaschek, and W. Kiefer, "A device for surface-scanning micro-Raman spectroscopy," *Appl. Spectrosc.*, **46**, 1331–1334 (1992).
 12. A. Bertoluzza, M. A. Battaglia, R. Simoni, and D. A. Long, "Vibrational spectroscopic studies of a new class of oligophosphate glasses of biological interest. II," *J. Raman Spectrosc.*, **14**, 178–183 (1983).
 13. H. Siebert, *Anwendungen der Schwingungsspektroskopie in der anorganischen Chemie*, Springer-Verlag, Berlin, 1966.
 14. F. A. Cotton, *Chemical Applications of Group Theory*, 2nd ed., Wiley Intersciences, New York, 1971.
 15. B. Dickens, W. E. Brown, G. J. Kruger, and J. M. Stewart, "Tetracalcium phosphate: Crystal structure and relationship to $\text{Ca}_5(\text{PO}_4)_3\text{OH}$ and $\text{K}_3\text{Na}(\text{SO}_4)_2$," *Acta Cryst.*, **29**, 2046–2056 (1973).
 16. W. E. Brown and E. F. Epstein, "Crystallography of tetracalcium phosphate," *J. Res. Natl. Bur. Stand.*, **69A**, 547–551 (1965).
 17. D. G. A. Nelson and B. E. Williamson, "Low-temperature laser Raman spectroscopy of synthetic carbonated apatites and dental enamel," *Aust. J. Chem.*, **35**, 715–727 (1982).
 18. R. I. Martin and P. W. Brown, "Hydration of tetracalcium phosphate," *Adv. Cement Res.*, **5**, 119–125 (1993).